2006

Quantum Dot Infrared Photodetector Fabricated by Pulsed Laser Deposition Technique

Mohammed Hegazy
Old Dominion University

Tamer Refaat

Nurul Abedin

Hani Elsayed-Ali
Old Dominion University, helsayed@odu.edu

Quantum-dot Infrared Photodetector Fabricated by Pulsed Laser Deposition Technique

Mohammed HEGAZY[*], Tamer REFAAT[**], Nurul ABEDIN[***] and Hani ELSAYED-ALI[*]

[*]*Old Dominion University, Physical Electronics Research Institute, Electrical and Computer Engineering Department, Norfolk, VA-23529*
E-mail: helsayed@odu.edu
[**] *NASA Langley Research Center, Science and Technology Corporation, Hampton, VA-23681*
[***] *NASA Langley Research Center, Passive Sensor Systems Branch, Hampton, VA-23681*

Pulsed laser deposition is used to fabricate multilayered Ge quantum-dot photodetector on Si(100). Growth was studied by reflection high-energy electron diffraction and atomic force microscopy. The difference in the current values in dark and illumination conditions was used to measure the device sensitivity to radiation. Spectral responsivity measurements reveal a peak around 2 μm, with responsivity that increases three orders of magnitude as bias increases from 0.5 to 3.5 V.

Keywords: Quantum, dots, infrared, detector, PLD

1. Introduction

Ge quantum dots (QD) are very promising for fabricating mid-infrared photodetectors [1,2], thermoelectric devices [3], and enhancing the performance of solar cells [4]. Unlike the case of single crystal photodetectors, controlling the QD size distribution, shape and density can be used to tune the device detection band [1,5]. Ge growth on Si follows the Stranski-Krastanow (SK) mode, in which Ge atoms form few epitaxial monolayers (wetting layer) before developing "self-assembled" QDs, in order to relief the strain caused by the lattice mismatch [6]. The amount of that strain and the deposition conditions control the shape, size and spatial distributions of the QDs; therefore allows for the tuneability of the detected wavelength band.

Ge QDs were grown on Si by molecular beam epitaxy (MBE) [7], chemical vapor deposition (CVD) [8], and liquid phase epitaxy (LPE) [2]. However, very few works have used pulsed laser deposition (PLD) to grow Ge on Si and to fabricate optical and electrical devices. PLD is one of the powerful techniques for growing thin films. Among its attractive features are the preservation of stoichiometry, the ease to grow multilayered films, the ability to grow thin films out of any material, the morphology-enhancing effect of the highly energetic deposited particles, and the periodic nature that allows for surface relaxation between pulses. The first two features would enable the growth of multilayered devices of different materials or dopings without the need for residual gases or doping sources; just targets with the desired doping are used. This should lead to a reduction in the fabrication time and cost.

In this work, PLD is used to fabricate a multi-layered infrared photodetector that is based on Ge QDs grown on Si(100) substrate.

2. Photodetector fabrication

A schematic of the deposition system is shown in Fig. 1. Si substrates are chemically cleaned prior being loading into the vacuum chamber [9]. The chamber is pumped down to a pressure of $<1\times10^{-8}$ Torr and baked for 12-24 hours before flashing the substrate to ~1100 ºC in order for the 2×1 reconstruction to develop. The Si substrate is kept at 773 K during deposition in a base pressure $<1\times10^{-9}$ Torr. A 40-ns Nd:YAG laser (0.16 J/cm², 50 Hz) is used to ablate the rotating target, which is in the form of two semi-circular disks placed together to form a circle; one is Si (p-type, 1×10^{19} cm⁻³) and the other is undoped Ge. During target rotation, PLD minimizes the formation of particulates by exposing a fresh area to the laser; thus, the probability of fracto-emission is minimized. The laser is focused on the rotating target with a spot size of 330 μm (measured at 1/e of the peak value). The system is designed in such a way that the laser can hit the target at 45°. A thickness of ~0.6 nm Ge is first deposited, followed by depositing ~0.4 nm Si. The process is repeated for 40 revolutions. A Si capping film of ~1 nm is deposited before a mask is used to deposit about 100-nm thick Al contacts. The deposition of the 40-layered device (consisting of 40 successive Ge QD layers separated by 39 Si spacing films and covered by a Si capping), without the metal contacts, took ~500 s, which is much less than the time needed to fabricate similar devices by other deposition techniques. A schematic diagram of the device is shown in Fig. 2.
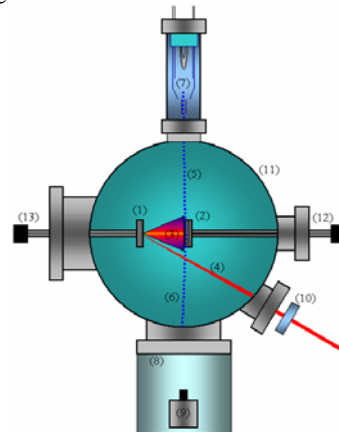

Fig. 1 A schematic diagram of the PLD system: (1) Target, (2) substrate (heated by direct current heating), (3) ablated species "Plume," (4) focused laser, (5) electron probe, (6) diffracted electrons, (7) electron gun, (8) phosphor screen, (9) CCD camera,

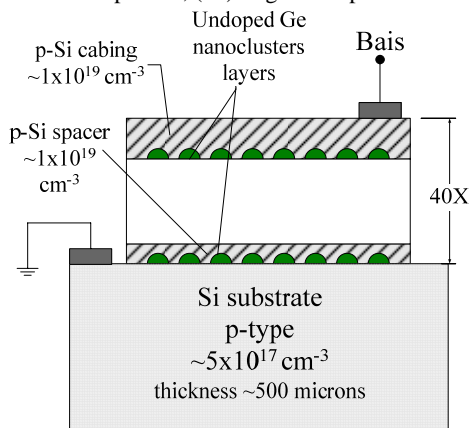(10) focusing lens, (11) ultrahigh vacuum chamber, (12) substrate manipulator, (13) target manipulator.

Fig. 2 Schematic diagram of the multi-layered Ge QD-based photodetector grown by PLD on Si(100).

3. Growth characterization

To *in situ* monitor the deposition, a 15-keV CW electron gun is used. A phosphor screen is used to display the electron diffraction pattern, which is recorded by a CCD camera. During the initial stages of deposition, the Si(100)-2×1, Fig. 3 (left), diffraction pattern does not change, which accounts for the formation of the 2D wetting layer. In such 2D growth, the Ge film grows having the Si lattice constant. Upon the completion of the first Ge layer, the RHEED diffraction pattern transforms into a transmission pattern, Fig. 3 (right), indicating the formation of Ge QDs. Ge QDs form to reduce the internal strain inside the film due to the lattice mismatch between Ge and Si. Such transmission pattern is taken as an indication for the formation of QD to start the deposition of the Si spacing film. As the capping film is being grown, the transmission pattern does not change in shape, but decreased in intensity.
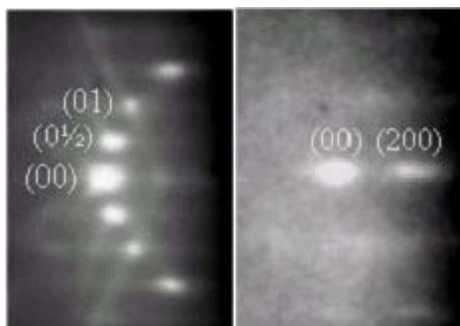

Fig. 3 (Left) RHEED diffraction pattern of the Si(100)-2×1 substrate. (Right) Transmission pattern formed when the growth of the first Ge QD layer is completed.

The morphology of the Ge film is studied by *ex situ* atomic force microscopy (AFM) (Digital Instruments; Nanoscope 3100). For this purpose, a Ge film, of the same thickness of the first QD layer, was grown under the same deposition conditions. Figure 4 shows the formation of the Ge QDs, which are distributed homogeneously over the substrate. A detailed study of the Ge QD formation on Si(100)-2×1 showed that, under similar deposition conditions at the same thickness hut clusters are formed [10].

The inset of Fig. 4 shows the QDs size (the length of the major axis) distribution that spans from 20 to 200 nm.

4. Electrical and optical characterization

Silver epoxy was used to mount the QD detector sample on an aluminum sample holder and to fix the connecting wires to the Al pads. Figure 5 shows a schematic of the characterization setup [11]. The setup consists mainly of optical, electrical and mechanical sections. The mechanical section is used to mount the device while conditioning its operation in terms of alignment, temperature and bias voltage. The sample holder was mounted on the cold-finger of a vacuum sealed cryogenic chamber (dewar). The chamber was cooled by liquid nitrogen and the required temperature was obtained using a temperature controller (Lake Shore; Autotuning Temperature Controller 330). The controller senses the temperature using Si diode (Lake Shore; DT-470) and change it using resistive heaters. Vacuum isolation (~ 10^{-6} Torr) was used with the chamber to preserve temperature stability using a vacuum pumping system (Pfeiffer; Vacuum Pump System TSU071E). For the spectral response measurements, an optical signal was applied to the detector using the optical section. The optical section consists of a current controlled (Optronic Laboratories; Programmable Current Source OL65A) radiation source (Halogen lamp) the output of which is modulated using an optical chopper and analyzed using a monochromator (Optronic Laboratories; Monochromator OL750-S). The electrical section was integrated to measure the device output for a certain operating condition. Lock-in amplifier (Stanford Research Systems; DSP Lock-in Amplifier SR850) was used to measure the output signal for a given radiation input. A spectrum analyzer (Stanford Research Systems; 2 Channel dynamic Signal Analyzer SR785) was used for noise measurements. A semiconductor characterization system (Keithly; 4200) was used for the I-V measurements. All these instrumentation are linked to a personal computer for data acquisition and control. The instruments are synchronized using the chopper controller. A preamplifier (Stanford Research Systems; SR570) is used to convert the detector current into voltage signal.
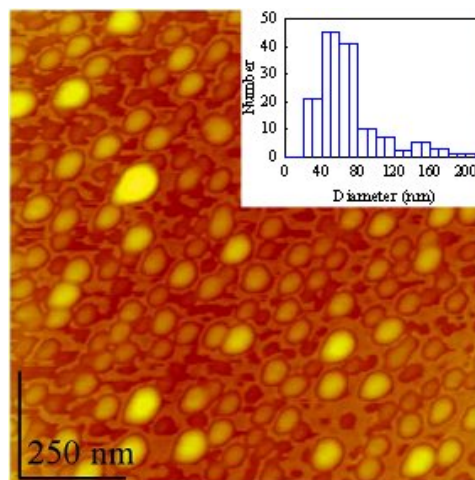

Fig. 4 AFM scan of the Ge quantum dots. The major axis length distribution is shown as inset [scan area = 1.1×1.1 μm].
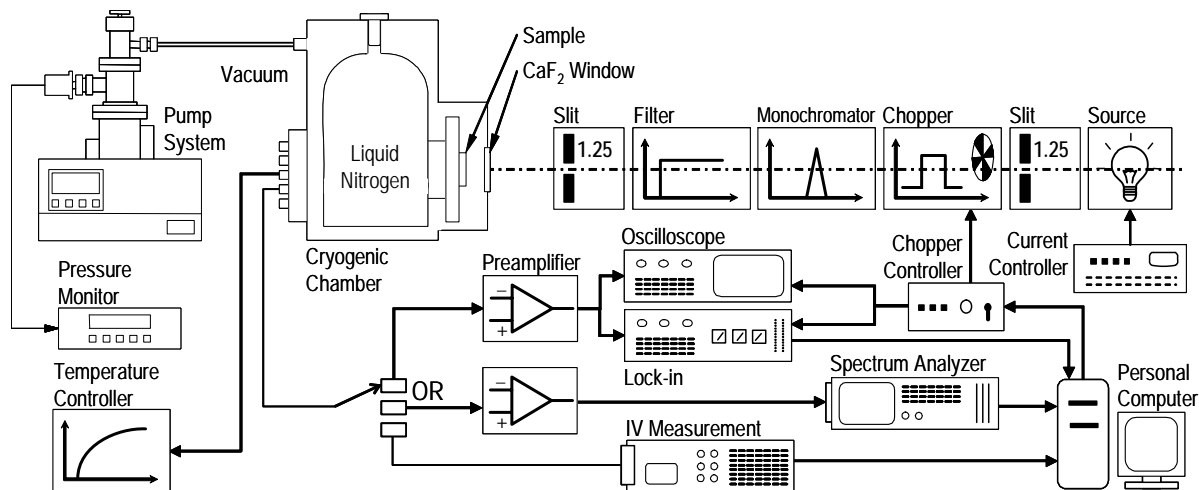
Fig. 5 A schematic of the detector characterization setup.

Figure 6 shows the I-V characteristics of the device at different operating temperatures. The I-V characteristics reveal the diode behavior of the sample, which confirms the Schottky structure. Cooling down the device slightly reduces the dark current, suggesting the domination of the leakage current due to the tunneling process. The inset of Fig. 6 zooms in to a part of the 293.2 K characteristics. The inset compares the curves obtained in dark and illumination conditions. A current shift of about 5 μA with 14.5 W/cm^2 incident intensity suggests the sensitivity of the device to radiation. In order to quantize this sensitivity a spectral response measurements were carried out.
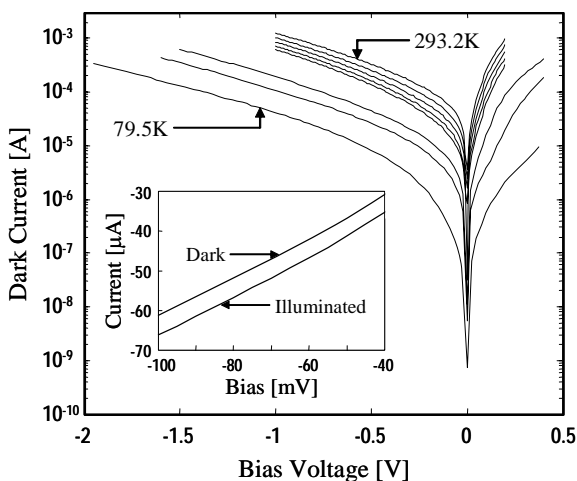

Fig. 6 Dark current variation with bias voltage obtained at temperatures of 293.2, 283.2, 273.2, 263.2, 253.2, 160.0, 130.0 and 79.5 K from top to bottom, respectively. The inset shows a portion of the dark current at 293.2 K and it variation due to device illumination with 14.5 W/cm^2 radiation intensity.

The spectral response of the QD photodetector sample is shown in Fig. 7. The characteristics assume 20-nm wavelength resolution with 10 averages. The characteristics were obtained in the wavelength range of 1.0 to 3.2 μm at 79.5 K operating temperature and different bias voltages. The spectral range is compatible with the optical section limitation. Lower temperatures have been used to minimize

the device noise since the responsivity is very low. The applied bias voltage was limited not to breakdown the device. The spectral response reveals peak responsivity around 2 μm wavelength with ~1.8 and ~2.2 μm cut-on and cut-off wavelengths, respectively. The presence of this peak is attributed to the type-II band lineup with interband transitions observed in Si/Ge QDs. Tuneability of this peak can be potentially achieved by controlling the composition, size, and size distribution of the QDs through varying the deposition parameters. These deposition parameters include growth temperature, laser fluence and repetition rate, and thickness of the Si spacers. PLD growth of Ge QDs and the control of their size and spatial distributions are reported elsewhere [10]. Another possible peak at a longer wavelength with a cut-on around 3 μm is visible in the figure. High responsivity at 1 μm dominates the maximum at 0.5 V due to absorption in the Si substrate. The responsivity increases almost three orders of magnitude (from ~5·10^{-6} A/W to ~3·10^{-3} A/W at 2 μm) by increasing the bias from 0.5 to 3.5 V. Although this might be attributed to an internal gain mechanism, it's associated with high increase in the noise level. This fact is clarified in Fig. 8, where the noise is plotted against the operating bias voltage. For comparison, the device detectivity (D*) is calculated and plotted in the same figure. Knowing the mean responsivity, $\Re$, at a certain bias voltage, and by measuring the noise current density, i_n, at the same voltage the detectivity is calculated using the relation

$$D* = \frac{i_n}{\Re} \cdot \sqrt{A} ,$$

where A is the area of the sensitive element. The figure reveals a poor detectivity compared to typical infrared detectors operating at the same wavelength range, even at room temperature. Nevertheless, the results indicate a promising device, with wavelength tunability option. The poor detectivity is attributed to the poor responsivity associated with QD detectors in general. Thus, research efforts should focus on-to the gain behavior and try to increase it.

In summary, the fabrication of a mid-infrared photodetector by PLD is reported. The device consists of 40 successive Ge QD layers separated by 39 Si spacers and

a topmost Si capping film. The fabrication time of the device, without the metal contacts, takes ~500 s. The growth was studied by *in situ* RHEED to identify the formation of Ge QDs, while *ex situ* AFM is used to study the morphology of the QDs and their size and spatial distributions. The difference in the current values in dark and illumination conditions shows the device sensitivity to radiation. Spectral responsivity measurements reveal a peak around 2 μm, the responsivity of which increases three orders of magnitude as the bias increases from 0.5 to 3.5 V. However, the low detectivity requires some design improvements.
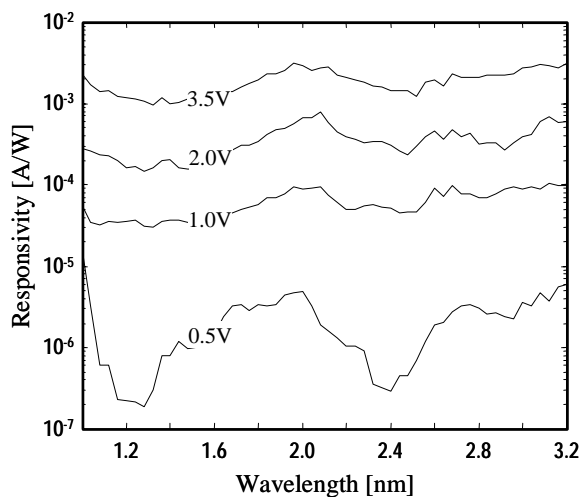

Fig. 7 Spectral response at different bias voltages, obtained at an operating temperature of 79.5 K.
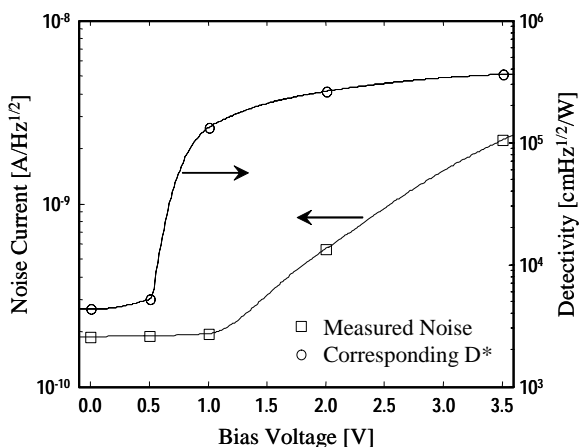

Fig. 8 Measured and fitted noise variation with bias voltage and the corresponding detectivity (D*), obtained at an operating temperature of 79.5 K.

References
[1] V. A. Egorov, G. É. Cirlin, A. A. Tonkikh, V. G. Talalaev, A. G. Makarov, N. N. Ledentosov, V. M. Ustinov, N. D. Zakharov, and P. Werner, Phys. Solid State **46**, 49 (2004).
[2] A. Elfving, G. V. Hansson, and W.-X. Ni, Physica E. **16**, 528 (2003).
[3] J. L. Liu, A. Khitun, K. L. Wang, T. Borca-Tasciuc, W. L. Liu, G. Chen, and D. P. Yu, J. Cryst. Growth **227-228**, 1111 (2001).
[4] A. Alguno, N. Usami, T. Ujihara, K. Fujiwara, G. Sazaki, K. Nakajima, and Y. Shiraki, Appl. Phys. Lett. **83**, 1258 (2003).
[5] C. Miesner, O. Röthing, K. Brunner, G. Abstreiter, Physica E **7**, 146 (2000).
[6] K. Brunner, Rep. Prog. Phys. **65**, 27-72 (2002).
[7] V. Cimalla, K. Zekentes, and N. Vouroutzis, Mater. Sci. Eng. B **88**, 186 (2002).
[8] P. S. Chen, Z. Pei, Y. H. Peng, S. W. Lee, M.-J Tsai, Mat. Sci. Eng. B **108**, 213 (2004).
[9] M. S. Hegazy and H. E. Elsayed-Ali, J. Vac. Sci. Tech. A **20**, 2068 (2002).
[10] M. S. Hegazy and H. E. Elsayed-Ali, Appl. Phys. Lett. 86, 243104 (2005).
[11] T. F. Refaat, M. N. Abedin, O. V. Sulima, U. N. Singh and S. Ismail, In IEDM Tech. Dig., page 355-358, 2004.